Supporting Information

Characterization of a Monocyanide Model of FeFe hydrogenase – Highlighting the Importance of the Bridgehead Nitrogen for Catalysis

C. Esmieu[a] and G. Berggren[a,*]

a Molecular Biomimetics, Department of Chemistry – Ångström Laboratory, Uppsala University, 75120 Uppsala, Sweden

Contents:

Table S1. Crystal data and structure refinement for compound **2**

Crystal data	
CCDC-No.	1437643
Empirical formula	$C_8H_5Fe_2N_2O_5S_2$, $C_8H_{20}N$
Formula weight	515.21
Crystal description	orange plate
Crystal size	0.2x0.18x0.08
Crystal system, space group	monoclinic, P 21/c
Unit cell dimensions: a	14.6311(5)
b	10.8642(4)
c	13.8535(4)
β	91.440(2)
Volume	2201.39(13)
Z	4
Calculated density	1.555
F(000)	1064
Linear absorption coefficient μ	1.538
Absorption correction	multi-scan, SADABS 2008
Max. and min. transmission	0.5857, 0.7455
Unit cell determination	$2.3 < \Theta < 25.2°$
	3585 reflections used at 100K
Data collection	
Temperature	100(2)K
Diffractometer	Bruker APEX-II CCD
Radiation source	fine-focus sealed tube
Radiation and wavelength	MoK_α, 0.71073Å
Monochromator	Graphite
Scan type	ω scans
Θ range for data collection	2.33 to 27.35°
Index ranges	$-15 \leq h \leq 18$, $-13 \leq k \leq 13$, $-14 \leq l \leq 17$
Reflections collected / unique	17828 / 4785
Significant unique reflections	3585 with $I > 2\sigma(I)$
R(int), R(sigma)	0.0575, 0.0608
Completeness to Θ_{max}	96.1 %
Refinement	
Refinement method	Full-matrix least-squares on F^2
Data / parameters / restraints	4785 / 318/ 0
Goodness-of-fit on F^2	1.053
Final R indices [$I > 2\sigma(I)$]	R1 = 0.0488, wR2 = 0.1143
R indices (all data)	R1 = 00.0703, wR2 = 0.1280
Weighting scheme	$w=1/[\sigma^2(F_o^2)+(aP)^2+bP]$ where $P=(F_o^2+2F_c^2)/3$
Weighting scheme parameters a, b	0.0494, 2.7603
Largest Δ/σ in last cycle	0.000
Largest difference peak and hole	1.237 and -0.895 e/Å³
Structure Solution Program	SHELXS-2014 (Sheldrick, 2008)
Structure Refinement Program	SHELXL-2014/7 (Sheldrick, 2008)

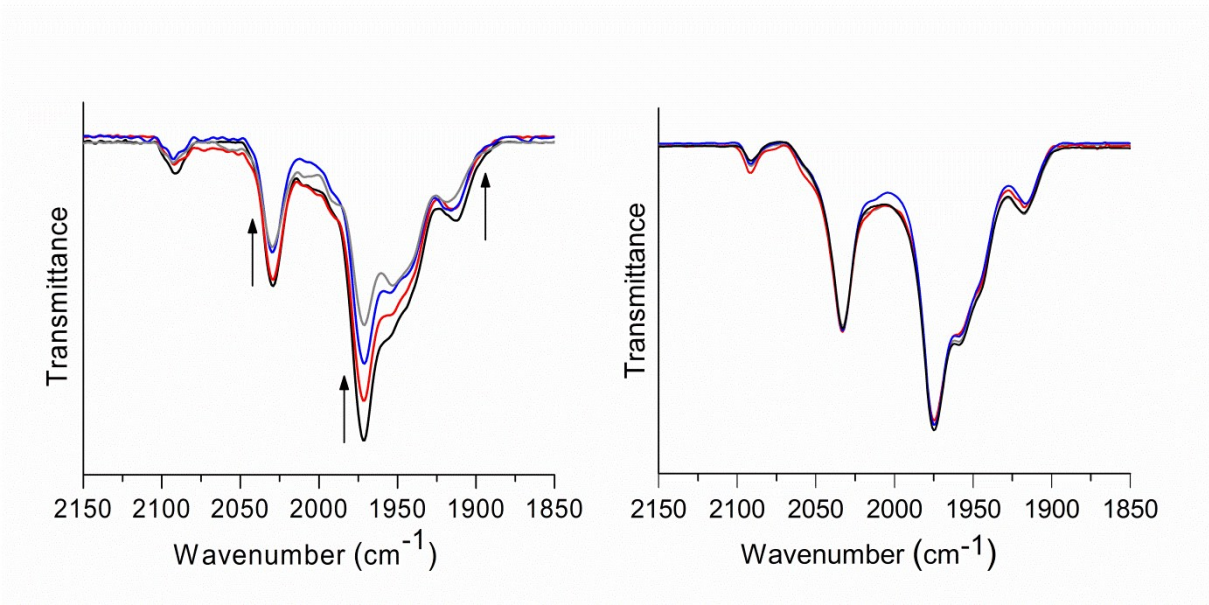

Fig. S1 The stability of complex **2** in anaerobic DMSO/H_2O (1:1) (left) and CH_3CN (right) solutions monitored by transmission FTIR spectropscopy. FTIR spectra recorded at t = 5 min (black line); t = 35 min (red line); t = 65 min (blue line); t = 125 min (grey line).

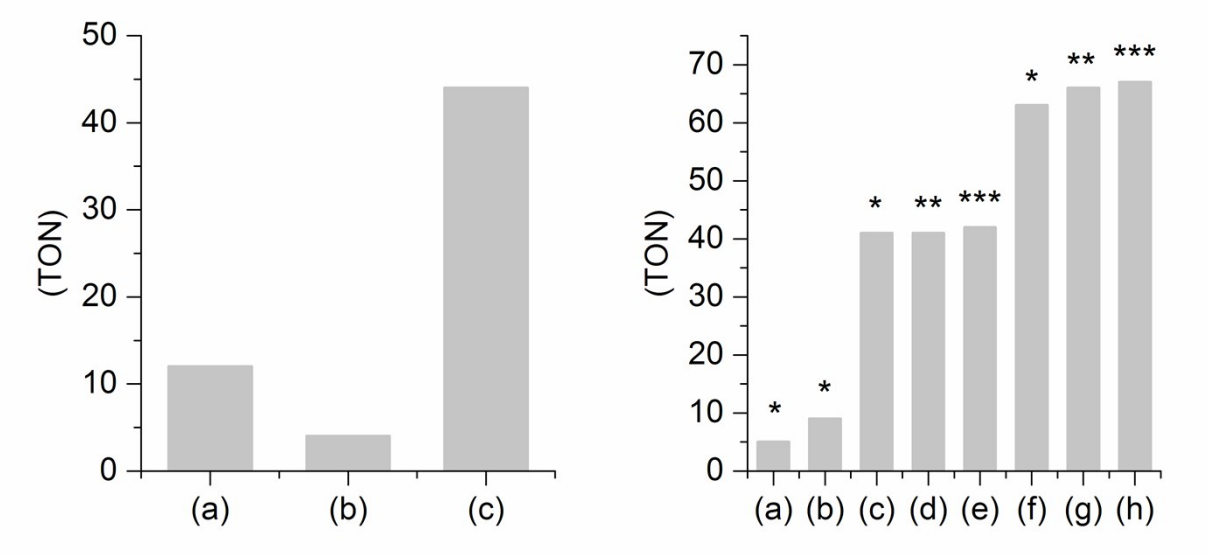

Fig. S2 The effect of changing buffer (left) and reaction time (right) on H_2 production observed following the addition of 39 μmoles of Eu-DTPA (final conc. 25 mM) to mixed DMSO/H_2O (1:1) solutions, H_2 amounts reported in TON relative to 0.39 μmoles catalyst (Fe^{2+} ions or complex **2**). Left: (a) blank; (b) $(NH_4)_2Fe(SO_4)_2$ (0.25 mM); (c) complex **2** (0.25 mM); Tris buffer 50 mM pH 7.5, V = 1.5 mL, 25 °C, after one hour reaction. Right: (a) blank ; (b) $(NH_4)_2Fe(SO_4)_2$ (0.25 mM); (c) complex **2** (0.25 mM); (d) complex **2** (0.25 mM); (e) complex **2** (0.25 mM); (f) complex **2** (0.25 mM) total H_2 production following a second addition of 39 μmoles Eu-DTPA; (g) complex **2** (0.25 mM) total H_2 production following a second addition of 39 μmoles Eu-DTPA; (h) complex **2** (0.25 mM) total H_2 production following a second addition of 39 μmoles Eu-DTPA. All Reactions performed in DMSO/H_2O (1:1) buffer (50 mM HEPES, pH 7.5), V = 1.5 mL, at 25 °C. * 1 h reaction time; ** 2 h reaction time time; *** 3 h reaction time.

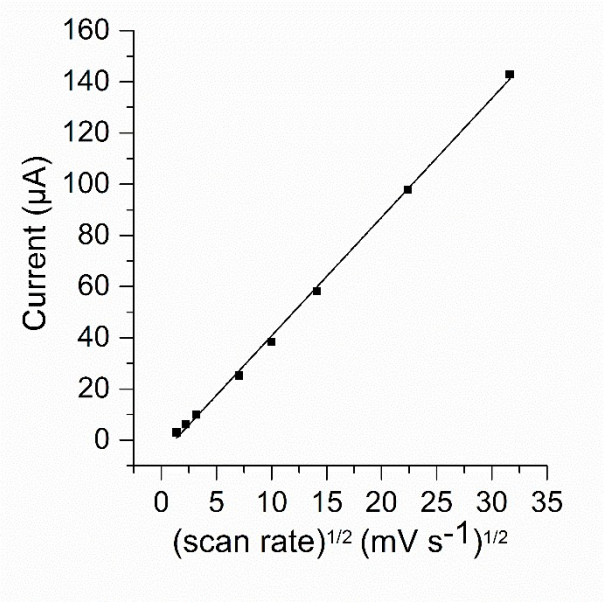

Fig. S3 Plot of anodic peak current ($i_{p,a}$) of complex **2** *vs* (scan rate)$^{1/2}$ from cyclic voltammetry. Conditions: 50 μM of **2** in CH_3CN-Bu_4NPF_6 (0.1 M); glassy carbon as working electrode with a surface area of 0.0701 cm^2.

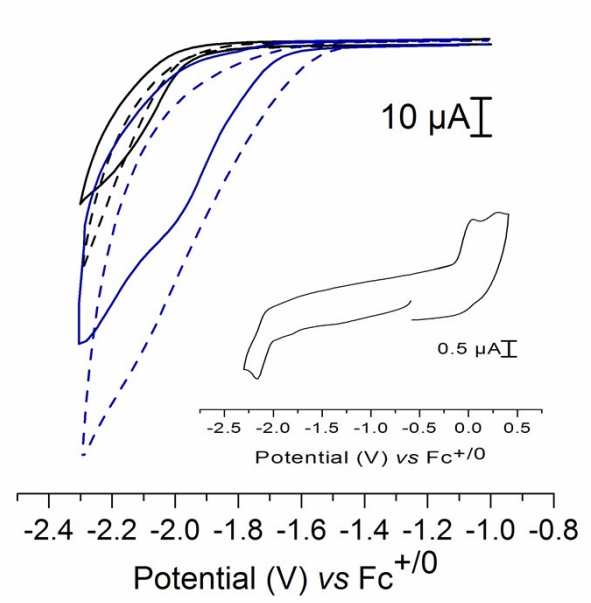

Fig. S4 Onset of catalytic current following addition of acid in the presence and absence of **3**, and cyclic voltammogram of **3** in pure electrolyte (inset). Complex **3** (50 μM) in presence of 6 mM acetic acid (black solid line) or 10 mM dichloroacetic acid (blue solid line); 10 mM acetic acid without complex **3** (dashed black line); 14 mM dichloroacetic acid without complex **3** (dashed blue line). Conditions: CH_3CN-Bu_4NPF_6 (0.1 M); scan rate = 100 mV s^{-1}; glassy carbon as working electrode with a surface area of 0.0701 cm^2. Cathodic peak current ($i_{p,c}$): −2.16 V; Anodic peak current ($i_{p,a}$): 0.05 V and 0.03 V

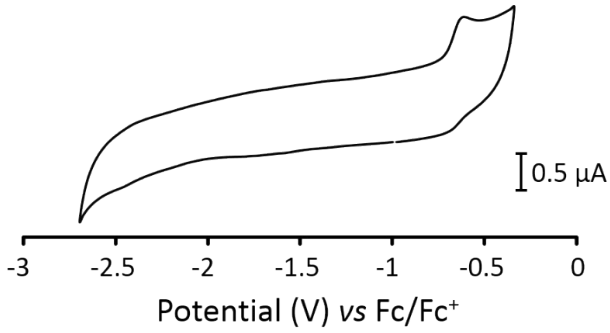

Fig. S5 Cyclic voltammogram of **1**. Conditions: 50 µM of **1** in CH_3CN-Bu_4NPF_6 (0.1 M); scan rate = 100 mV s^{-1}; glassy carbon as working electrode with a surface area of 0.0701 cm^2.

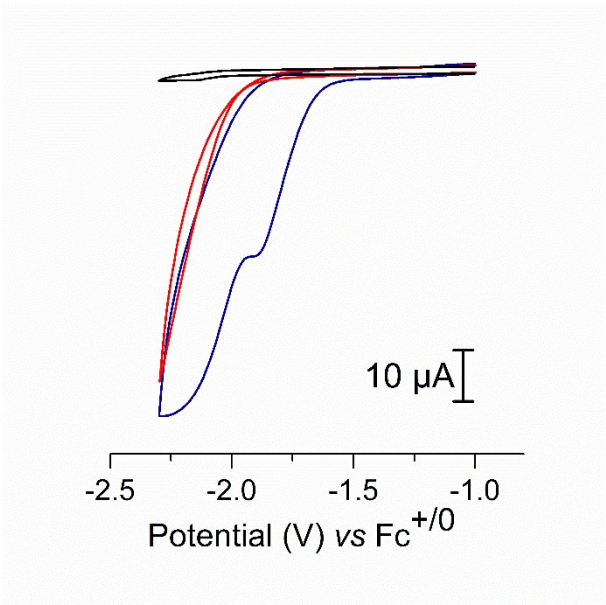

Fig. S6 Onset of catalytic current following addition of acetic acid in the presence and absence of **2.** Complex **2** (50 µM) in pure electrolyte (black); complex **2** (50 µM) in presence of 10 mM acetic acid (blue); 10 mM of acetic acid without complex (red). Conditions: CH_3CN-Bu_4NPF_6 (0.1 M); scan rate = 100 mV s^{-1}; glassy carbon as working electrode with a surface area of 0.0701 cm^2.

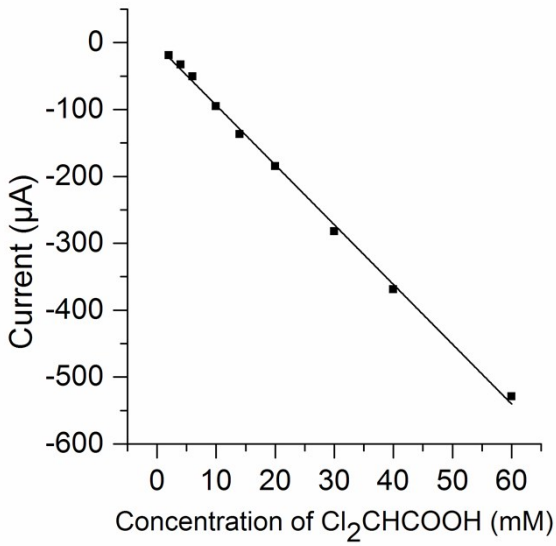

Fig. S7 Plot of cathodic peak current ($i_{p,c}$) of complex **2** *vs* the acid concentration from cyclic voltammogram. Conditions: 50 μM of **2** in CH_3CN-Bu_4NPF_6 (0.1 M); scan rate = 100 mV s^{-1}; glassy carbon as working electrode with a surface area of 0.0701 cm^2.

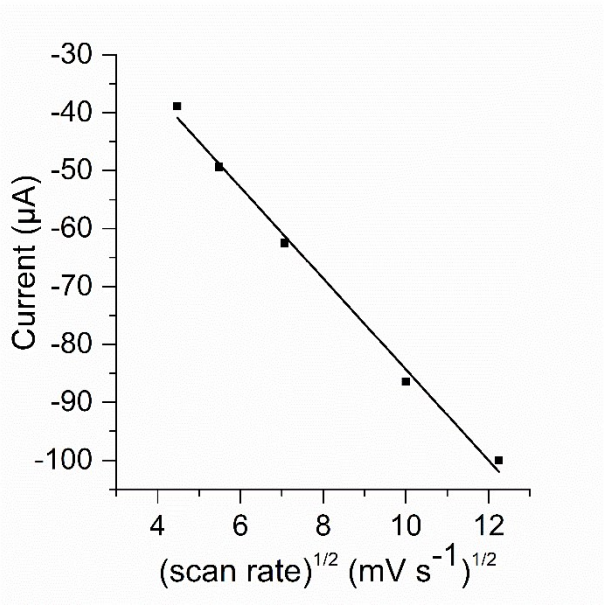

Fig. S8 Plot of cathodic current (at -1.7 V) of complex **2** *vs* (scan rate)$^{1/2}$ in the presence of dichloroacetic acid from cyclic voltammetry. Conditions: complex **2** (50 μM) and Cl_2AcOH (10 mM) in CH_3CN-Bu_4NPF_6 (0.1 M); glassy carbon as working electrode with a surface area of 0.0701 cm^2.

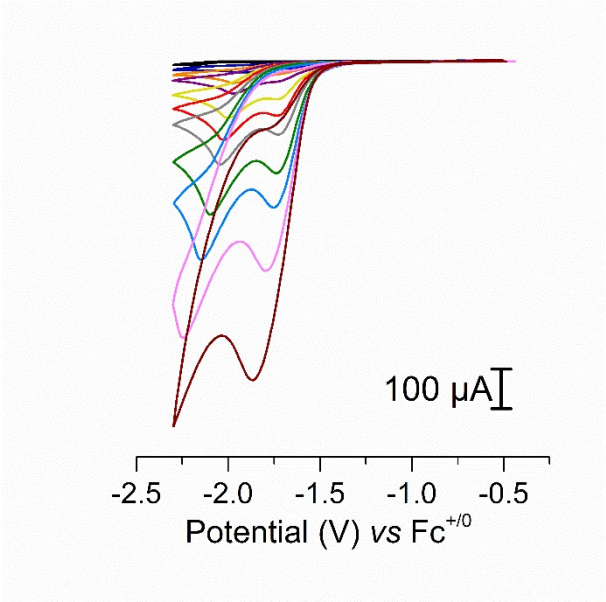

Fig. S9 Cyclic voltammograms of **2** in the presence of increasing amounts of dichloroacetic acid from 0 (black) to 500 (brown) equivalents. Conditions: 200 μM of **2** in CH_3CN-Bu_4NPF_6 (0.1 M); scan rate = 100 mV s^{-1}; glassy carbon as working electrode with a surface area of 0.0701 cm^2.

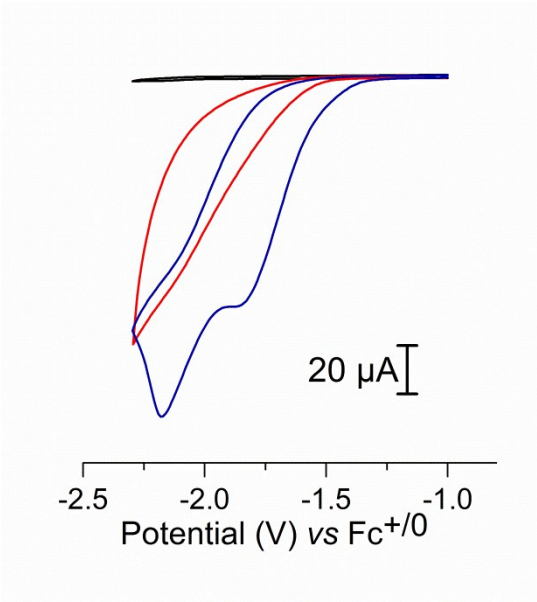

Fig. S10 Onset of catalytic current following addition of dichloroacetic acid in the presence and absence of **2.** Complex **2** (50 μM) in pure electrolyte (black); complex **2** (50 μM) in presence of 10 mM of dichloroacetic acid (blue); 10 mM of dichloroacetic acid without complex (red). Conditions: CH_3CN-Bu_4NPF_6 (0.1 M); scan rate = 100 mV s^{-1}; glassy carbon as working electrode of surface area 0.0701 cm^2.

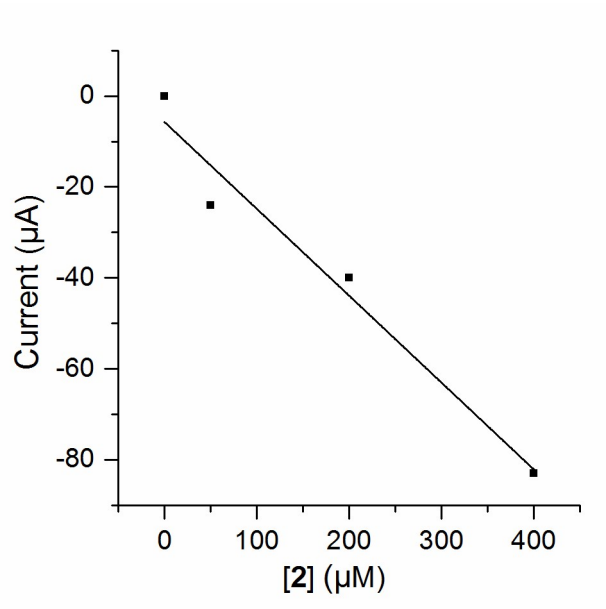

Fig. S11 Plot of cathodic current (at −1.68 V) of complex **2** *vs* the catalyst concentration from cyclic voltammogram. Currents corrected by subtracting background current observed for dichloroacetic acid. Conditions: 20 mM of dichloroacetic acid in CH_3CN-Bu_4NPF_6 (0.1 M); scan rate = 100 mV s^{-1}; glassy carbon as working electrode with a surface area of 0.0701 cm^2.

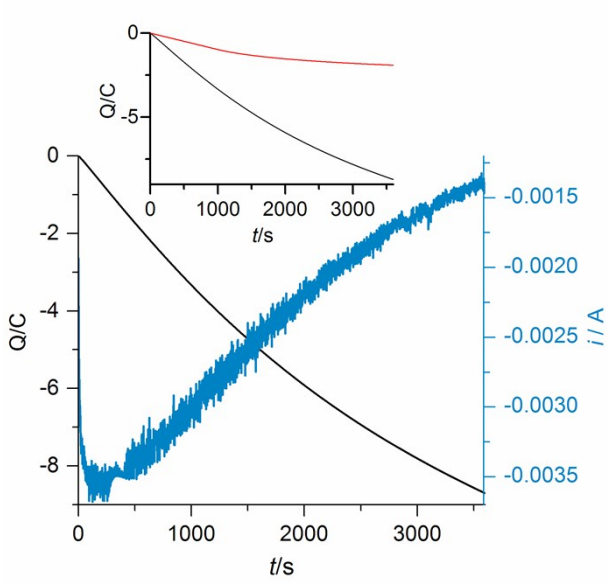

Fig. S12 Controlled potential coulometry of **2** (0.5 mM) in the presence of dichloroacetic acid, charge (Q, black line) passed through the cell and current (*i*, blue line) shown as a function of time; (inset): Charge passed through the cell in the presence (black line) and absence (red line) of **2**. Conditions: 50 mM of dichloroacetic acid in CH_3CN-Bu_4NPF_6 (0.1 M); glassy carbon as working electrode with a surface area of 0.22 cm^2; potential set to −1.7 V.

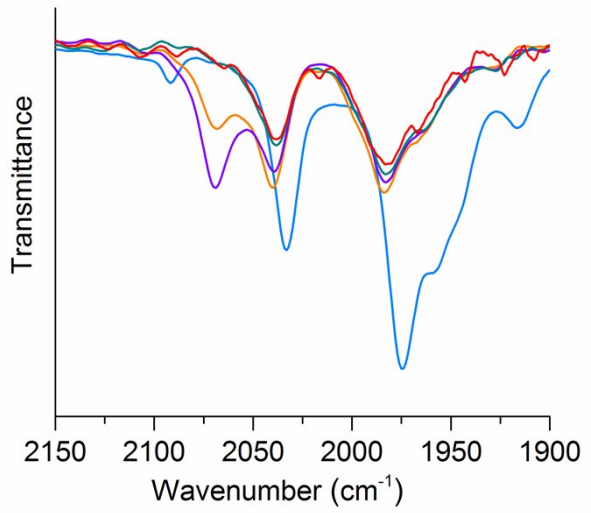

Fig. S13 The stability of complex **2** under electrocatalytic conditions monitored by transmission FTIR spectropscopy. Samples collected and transferred *via* syringe to the sample cell, FTIR spectra recorded at t = 0 s (blue); t = 300 s (orange); t = 1800 s (violet); t = 3600 s (green); t = 7200 s (red). Conditions: 0.5 mM **2**; 50 mM of dichloroacetic acid in CH_3CN-Bu_4NPF_6 (0.1 M); glassy carbon as working electrode with a surface area of 0.22 cm^2; potential set to −1.7 V.

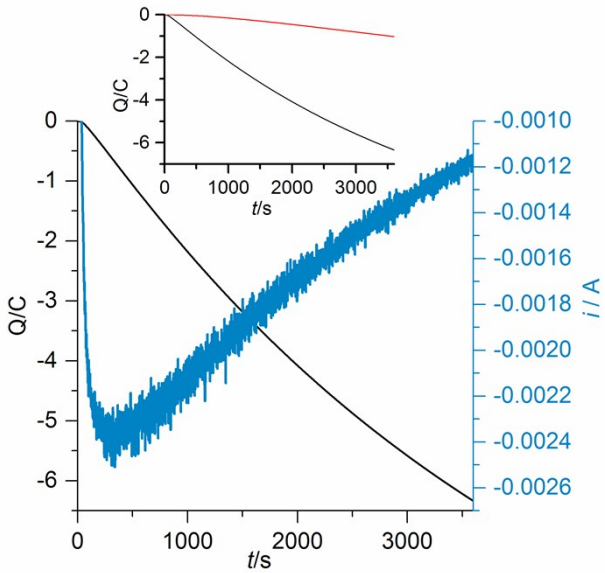

Fig. S14 Controlled potential coulometry of **2** (0.5 mM) in the presence of acetic acid, charge (Q, black line) passed through the cell and current (*i*, blue line) shown as a function of time; (inset): Charge passed through the cell in the presence (black line) and absence (red line) of **2**. Conditions: 50 mM of acetic acid in CH_3CN-Bu_4NPF_6 (0.1 M); glassy carbon as working electrode with a surface area of 0.22 cm^2; potential set to −1.8 V.